Lignosulfonamides as a new group halogen free flame retardant for PLA

Tomasz M. Majka[1), *)] (ORCID ID: 0000-0002-7913-0750)**, Zuzanna Zawadzka[1)], Radosław Piech[1)]**

DOI: https://doi.org/10.14314/polimery.2024.11.7

Abstract: Dibutyl-lignosulfonamide (DBA), *N*-butyl-*N*-dodecyl-lignosulfonamide (NNA) and didodecyl-lignosulfonamide (DDA) were used as halogen-free flame retardants (HFFR) of PLA. Lignosulfonamides were used in amounts of 3, 6 and 9 wt%. The composites were analyzed by TGA, DSC and micro-combustion calorimetry (MCC). Lignosulfonamides were shown to reduce PLA flammability by up to 40%. The lowest flammability was obtained with the highest HFFR content. The reduction in flammability can be explained by the release of SO_2 at the early stage of biocomposite decomposition, which promotes the formation of coke and char, acting as a local insulator.

Keywords: calcium lignosulfonate, flame retardants, flammability, biopolymers, PLA.

Lignosulfonamidy jako nowa grupa bezhalogenowych środków zmniejszających palność PLA

Streszczenie: Dibutylo-lignosulfonamid (DBA), *N*-butylo-*N*-dodecylo-lignosulfonamid (NNA) i didodecylo-lignosulfonamid (DDA) użyto jako bezhalogenowe środki obniżające palność (HFFR) PLA. Lignosulfonamidy stosowano w ilości 3, 6 i 9 % mas. Kompozyty poddano analizie TGA, DSC oraz mikrokalorymetrii spalania (MCC). Wykazano, że lignosulfonamidy zmniejszają palność PLA nawet o 40%. Najmniejszą palność uzyskano przy największej zawartości HFFR. Zmniejszenie palności można wyjaśnić wydzielaniem się SO_2 na wczesnym etapie rozkładu biokompozytów, który promuje powstawanie koksu i zwęgliny, działających jak miejscowy izolator.

Słowa kluczowe: lignosulfonian wapnia, środki zmniejszające palność, palność, PLA.

Halogen-free flame retardants (HFFR), like traditional flame retardants, are used to increase the fire resistance of polymeric and biopolymeric materials. The essence of their use is the absence of halogens, making them more environmentally friendly [1, 2]. The use of green HFFRs also makes it possible to meet stringent safety standards without burdening the environment. In addition, they are more compatible with biopolymers, to which they can be bound in many ways, e.g., grafting, adsorption, and physical mixing [3, 4]. Their continued improvement is driven by concerns about the environmental and health effects of halogen compounds. This is because traditional flame retardants produce harmful volatile compounds during combustion, which later persist in ecosystems. Thus, the search for HFFR represents a safer approach to reducing the flammability of materials as part of sustainable development [5, 6].

Organo-sulfur compounds with sulfur-nitrogen bonds are such an example. Among them, 3 types of compounds should be distinguished: sulfenamides, sulfinamides, and sulfonamides. Sulfenamides, due to their high S-N bond instability, are widely used as vulcanization accelerators in the rubber industry [7, 8]. In contrast, sulfinamides are used only as an auxiliary agent in organic synthesis, e.g., derivatives of amines, cyclopentanes, ethers [9–12]. Meanwhile, sulfonamides are a family of organosulfur compounds that are commonly used as colorants and plasticizers for composite materials [13–15]. Prof. Bahrami's team published reports in 2019 on work on the two-step synthesis of sulfonamides in one pot from the corresponding thiols and amines by oxidative chlorination of thiols to sulfonyl chlorides, followed by reaction with amines [16, 17]. Inspired by these works, in 2023, Majka proposed a two-step method for the synthesis of lignosulfonamides by modifying calcium lignosulfonate to lignosulfonyl chloride and then reacting it with a secondary amine [18]. The successively obtained lignosulfonamides were evaluated for thermal stability and flammability. As a result of the four different synthesis routes proposed for lignosulfonyl chloride in the first step, and the three types of amines used (dibutyl-

[1)] Cracow University of Technology, Department of Chemistry and Technology of Polymers, ul. Warszawska 24, 31155 Kraków, Poland.

[*)] Author for correspondence: tomasz.majka@pk.edu.pl

amine, *N*-butyl-*N*-dodecylamine, and didodecylamine) in the second step, only the lignosulfonamides obtained using PCl_5 (Route B) had negligible flammability and better thermal stability. It was then concluded that the obtained compounds could be used as flame retardants for biocomposites.

The aim of this work was to synthesize lignosulfonamides and use them as halogen-free flame retardants for PLA. The obtained PLA composites differing in lignosulfonamide content were studied for thermal stability, phase transformations and flammability using thermogravimetric thermal analysis (TGA), differential scanning calorimetry (DSC), and micro-combustion calorimetry (MCC).

EXPERIMENTAL PART

Materials

Polylactide (PLA), with the trade name Ingeo™ Biopolymer 3052D was purchased from NatureWorks (Blair, USA). Calcium lignosulfonate with the trade name Lignobind type 1 (CLS) was supplied by Penquisa (Beriain, Spain). PCl_5, dibutylamine, *N*-butyl-*N*-dodecylamine and didodecylamine were obtained from Sigma Aldrich (Darmstadt, Germany).

Lignosulfonamides synthesis

The process of obtaining lignosulfonamides was carried out in two stages, as described in [18]. The first stage consisted of the reaction of calcium lignosulfonate (CLS) with PCl_5 to obtain lignosulfonyl chloride, which in the second stage reacted with secondary amines having in their structure: a) two short aliphatic chains of 4 carbon atoms (dibutylamine), b) one short aliphatic chain of 4 carbon atoms and one long aliphatic chain of 12 carbon atoms (*N*-butyl-*N*-dodecylamine) and c) two long aliphatic chains of 12 carbon atoms (didodecylamine). Dibutyl-lignosulfonamine (DBA), *N*-butyl-*N*-dodecyl-lignosulfonamine (NNA), and didodecyl-lignosulfonamine (DDA) obtained in this way were used to receive biocomposites by high-temperature extrusion.

Composites preparation

A laboratory twin-screw miniCTW extruder (Thermo Scientific, Poznań, Poland) was used in the preparation of PLA biocomposites (Figure 1). Using this co-rotating conical-screw extruder, PLA/CLS, PLA/DBA, PLA/NNA, and PLA/DDA composites containing 3, 6, and 9 wt% lignosulfonamides, respectively, were obtained. The process was carried out at 220°C, using a screw speed of 50 rpm, without degassing. The residence time was 7 min.

Methods

The thermogravimetric analysis (TGA) was performed using a Netzsch TG 209F1 Libra (Netzsch, Selb, Germany) apparatus. The test was conducted in an oxidizing atmosphere in the temperature range 25-600°C and heating rate 10°C/min. The differential scanning calorimetry (DSC) measurements were evaluated using a Mettler Toledo DSC823e (Mettler Toledo, Columbus, USA) apparatus. This measurement was conducted in an inert atmosphere according to the following temperature programs:

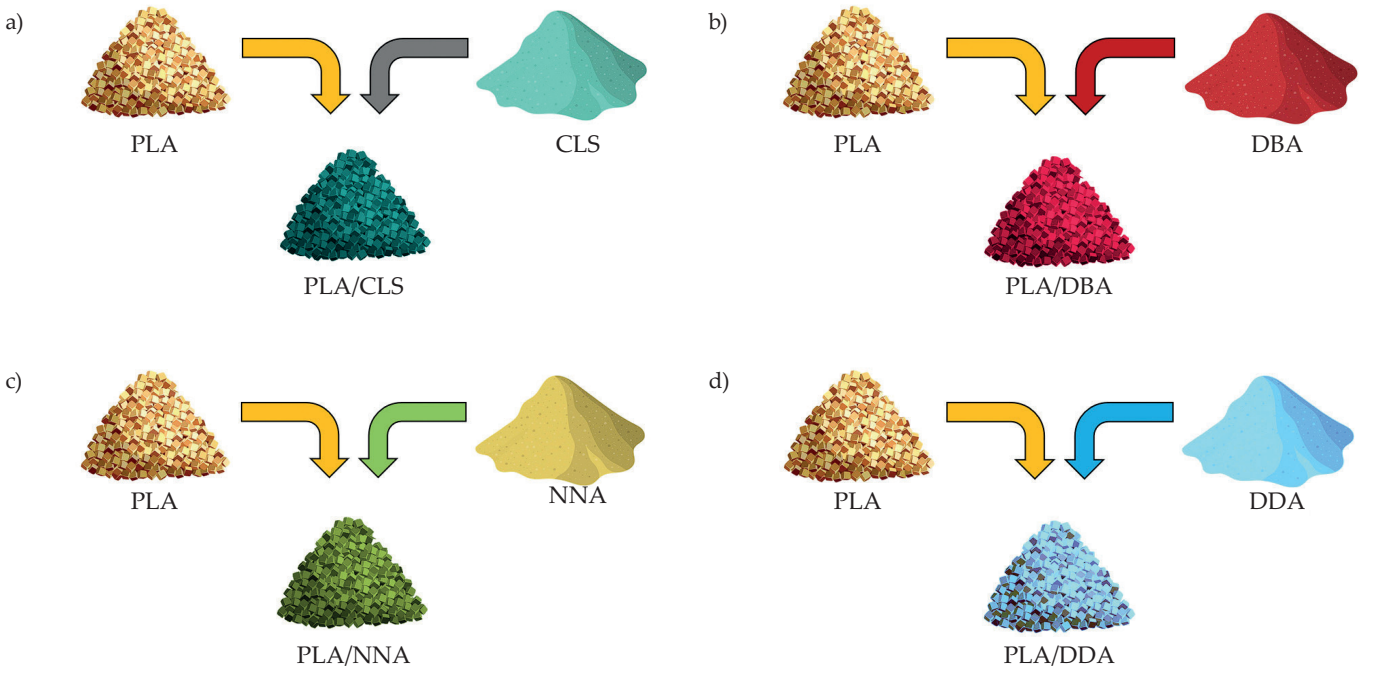

Fig. 1. Schematic diagram of PLA biocomposites preparation

– heating 25–180°C at a rate of 10°C/min,
– cooling 180–25°C at a rate of 10°C/min,
– heating 25–180°C at a rate of 10°C/min.

The micro-combustion calorimetry (MCC) was carried out using a fire testing technology (FTT, East Grinstead, UK) apparatus in accordance with ASTM D7309. Composite tests were conducted in the temperature range of 150–750°C at a heating rate of 1°C/s.

RESULTS AND DISCUSSION

Thermogravimetric analysis

As shown in [18], the CLS decomposition process occurred in two stages, where the first mass loss was observed at a temperature of about 206°C, and the next one in the temperature range of 360–400°C. In the literature [19, 20] a 3-stage decomposition process is also known, including loss of adsorbed water (30–150°C), volatilization of CO, CO_2, SO_2, mercaptans, and water of dehydration (150–400°C) and condensation reactions and secondary cracking of phenolic compounds (above 400°C). According to the literature [21], five groups of low molecular weight compounds are formed because of CLS decomposition: esters, guaiacols, phenolics, syringols, and other types. The use of *N*-butyl-*N*-dodecylamine. and didodecylamine allowed lignosulfonamides to be obtained with higher thermal stability than the starting CLS [18]. It is worth noting that during heating, the above amines decompose into CO, CO_2, hydrocarbons, nitrogen oxides, and amine vapors [22].

Figure 2 shows the thermogravimetric curves of PLA/DBA, PLA/NNA, and PLA/DDA composites divided into lignosulfonamide content. This analysis shows that all examined composites display a different trend of mass loss at the $T_{5\%}$ point (Table 1). Nevertheless, at the processing temperature of PLA, no more than 2% of the mass was lost. Regardless of the mass fraction of the filler,

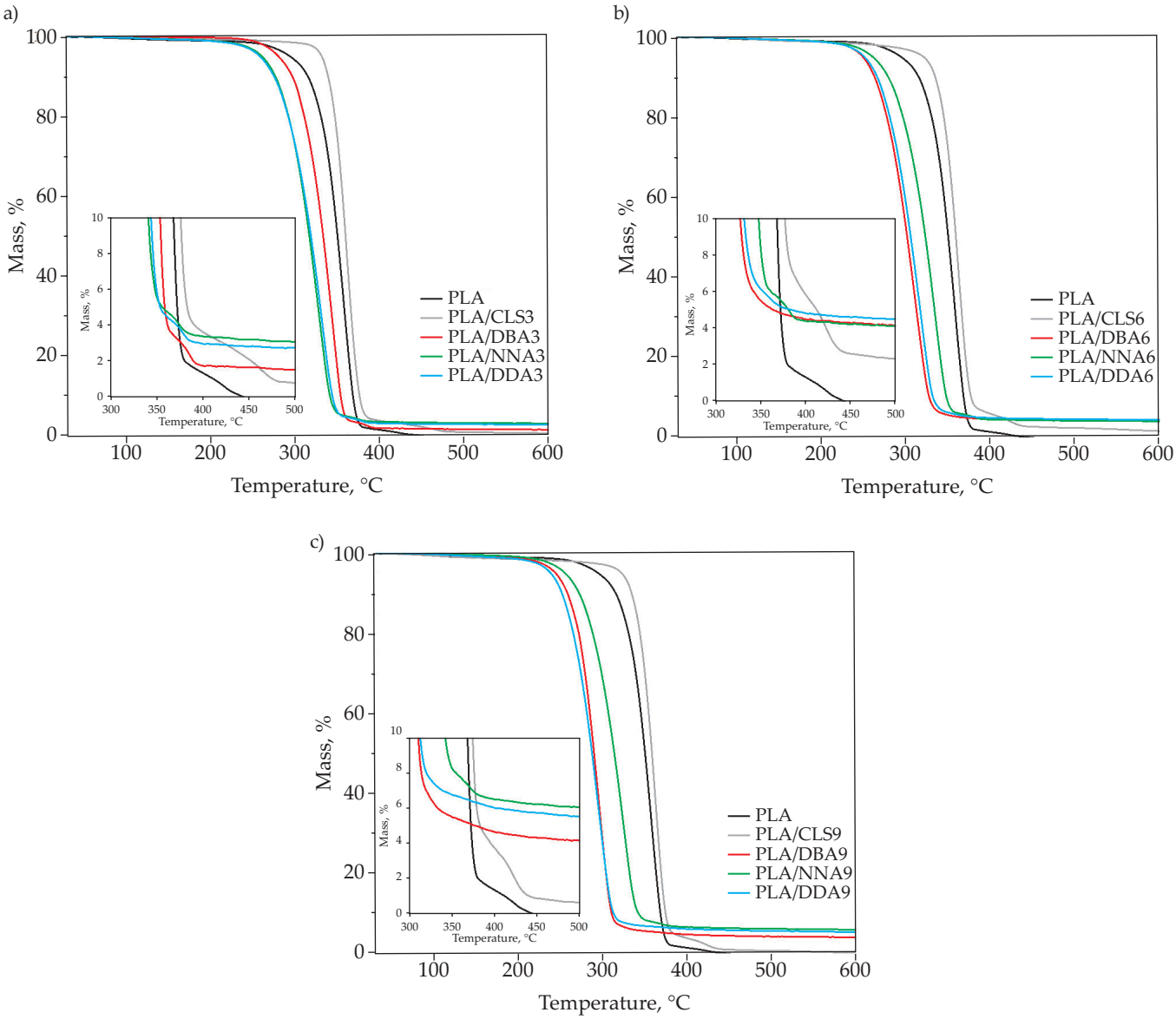

Fig. 2. TGA curves for PLA composites with different lignosulfonamide content: a) 3 wt%, b) 6 wt%, c) 9 wt%

T a b l e 1. TGA data for PLA hybrid biomaterials

Sample	$T_{5\%}$, °C	$T_{10\%}$, °C	$T_{20\%}$, °C	$T_{50\%}$, °C	T_{MAX}, °C	Residue at 600°C, %
PLA	294	314	330	350	358	0.00
PLA/CLS3	332	339	347	350	361	0.46
PLA/CLS6	321	335	345	359	362	1.52
PLA/CLS9	322	334	344	358	362	0.01
PLA/DBA3	280	296	310	333	345	1.35
PLA/DBA6	249	262	277	301	310	3.94
PLA/DBA9	243	257	271	289	295	3.90
PLA/NNA3	260	276	292	316	329	2.94
PLA/NNA6	260	278	296	323	335	3.94
PLA/NNA9	254	271	287	313	323	5.81
PLA/DDA3	258	274	291	318	326	2.60
PLA/DDA6	250	265	280	305	318	4.31
PLA/DDA9	237	251	264	287	296	5.20

the highest thermal stability was shown by composites containing CLS. The first stage of PLA/CLS samples decomposition occur at 362°C, while the second stage at 461°C for the PLA/CLS3 composite and at 421°C for the PLA/CLS6 and PLA/CLS9 composites. These results show that the amount of filling influenced the area of occurrence of the second phase of composite decomposition. Nevertheless, the decomposition of PLA/CLS composites allowed obtaining the smallest amount of residue at 600°C among all tested biocomposites.

Among the composites containing 3 wt% of HFFR, the highest thermal stability was demonstrated by PLA/DBA3, followed by PLA/NNA3 and PLA/DDA3. Thus, with the increase in the length of aliphatic chains in the structure of lignosulfonamides, the thermal stability of PLA composites with their participation gradually decreased. This also resulted in a shift of two stages of decomposition towards lower temperatures. At the same time, with the decrease in thermal stability, the content of residues after decomposition increased (Table 1).

Increasing lignosulfonamide content to 6 wt% resulted in the disappearance of the second stage of decomposition among the PLA/DBA6 and PLA/DDA6 composites. These composites displayed a similar thermal stability with a single-step decomposition mechanism, but thermal stability for them were lower than the PLA/NNA6 composite. Similar conclusions were drawn after analyzing the composites containing 9 wt% of lignosulfonamide. Also, among examined samples, the highest thermal stability was observed for the material decomposing in two stages (PLA/NNA9).

Based on the thermogravimetric analysis, the tested biomaterials were ranked in terms of thermal stability as following: PLA/CLS3 > PLA/CLS6 > PLA/CLS9 > PLA > PLA/DBA3 > PLA/NNA6 > PLA/NNA3 > PLA/DDA3 > PLA/NNA9 > PLA/DDA6 > PLA/DBA6 > PLA/DBA9 > PLA/DDA9. This order shows that the thermal stability of PLA/lignosulfonamide composites was influenced not only by the type of lignosulfonamide used but also by its amount. It is worth noting that samples which form larger amount of char residue during the main stage of decomposition occupy the last places in this ranking. In turn, biomaterials in which the process of char formation and its afterburning were separated as a second step and shifted towards higher temperatures were consequently characterized by higher thermal stability and low residue after decomposition.

DSC vs TGA

Figure 3 shows DSC curves compiled with TGA thermograms. In the range of three phase transformations the mass loss did not exceed 1.5 %. With the decreasing amount of lignosulfonamides in the PLA matrix, the degree of mass loss in the considered range also decreased, so that biocomposites containing 3 wt% of lignosulfonamide did not exceed 1%. The DSC indices obtained from this analysis are summarized in Table 2, with the degree of crystallinity calculated using Equation 1 [23, 24]**:**

$$X_C = \frac{\Delta H_m - \Delta H_{CC}}{(1 - \omega) \cdot \Delta H^o} \quad (1)$$

where ΔH_m – change in melting enthalpy of a polylactide sample, ΔH_{CC} – change in enthalpy of cold crystallization, ΔH^o – change in melting enthalpy of a completely crystalline polylactide equal to 93 J/g [24, 25], ω – HFFR content.

Three-phase transition steps were observed in the 30–180°C temperature range: glass transition, cold crystallization, and melting. It was found that the glass transition temperature (T_g) of biocomposites was influenced by the type and amount of lignosulfonamide. For example, T_g gradually decreased with increasing HFFR content for PLA/CLS and PLA/DBA composites. This fact is confirmed by the read values of the heat capacity (ΔC_p) (Table 2). These observations indicate that the addition of HFFR facilitated the transition from the glass to the

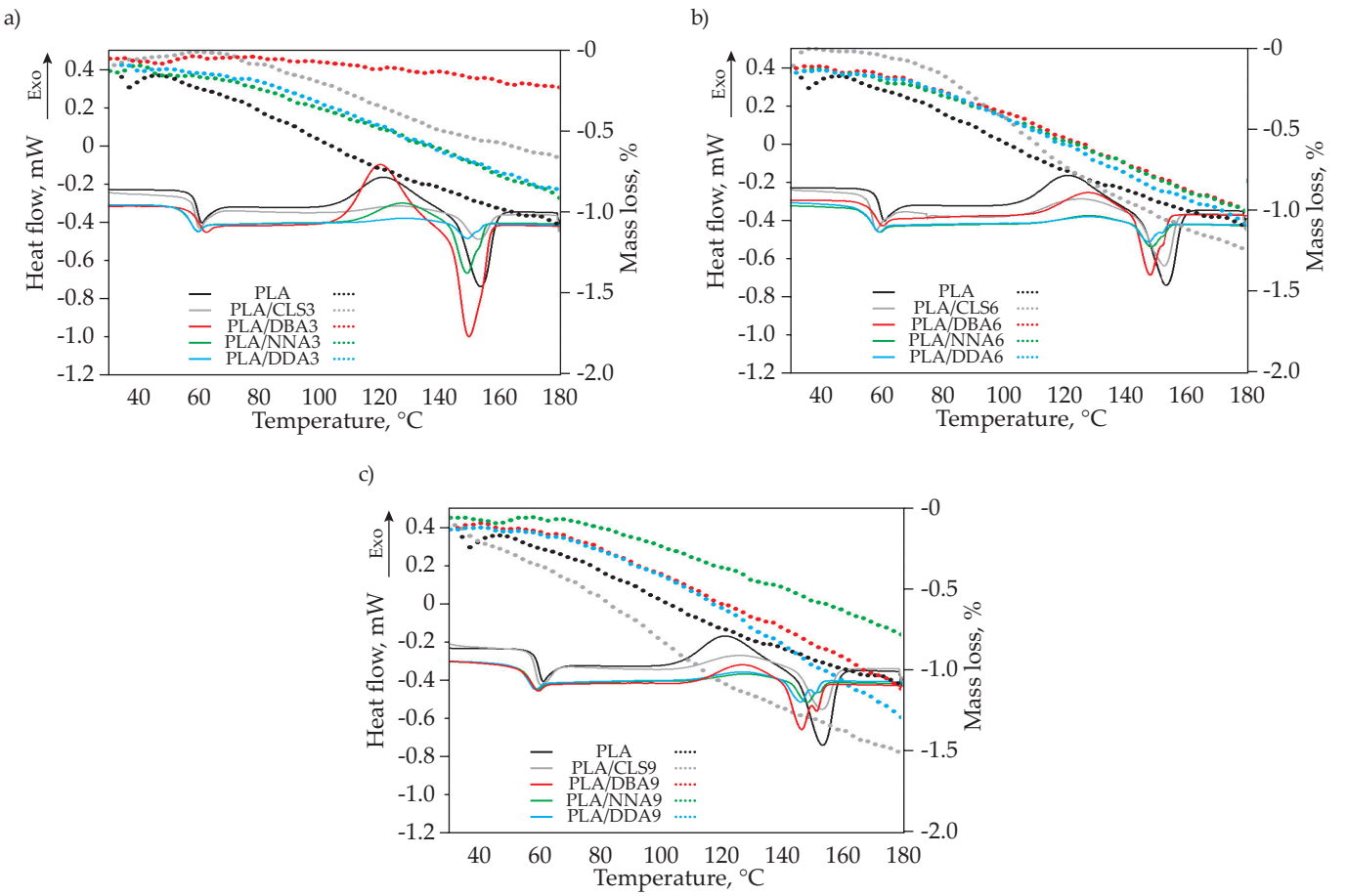

Fig. 3. DSC vs TGA curves for PLA biocomposites with different lignosulfonamide content: a) 3 wt%, b) 6 wt%, c) 9 wt%

plastic state, as significantly less heat had to be supplied to the system to reach the transition point between these two states. It is also concluded that the type of lignosulfonamide used played a minor role in this case. Referring to the TGA curves, it can be stated that at the T_g point for the samples containing 3 and 6 wt% of HFFR, the first inflection of the line was visible, suggesting the beginning of a slow process of mass loss.

HFFR did not affect the cold crystallization process of examined composites. On the other hand, PLA/lignosulfonamide composites showed a higher, cold crystallization temperature (T_{cc}) than PLA/CLS composites and the reference sample (PLA), with the sample containing 3 wt% dibutyl-lignosulfonamide being the only exception.

It can be concluded that the type of lignosulfonamide introduced affected the intensity of the cold crystallization peak. As a rule, composites containing DBA showed a much higher peak on the DSC curve than samples containing NNA, DDA, and even CLS. The samples were characterized by a double melting behavior. PLA, PLA/CLS composites, and the PLA/DBA3 sample were characterized by a single melting peak at approx. 153°C. As shown in Author another work [20], this is related to the formation of a dominant and stable α phase. These biomaterials were characterized by a high degree of X_c crystallinity. Both the increase in the amount of DBA in the composite above 3 wt% or the change of lignosulfonamide to other with longer aliphatic chains in its structure (NNA, DDA), led to the appearance of an additional, less stable α' phase, melting at about 148°C. Thus, all biocomposites characterized by two melting peaks had significantly lower X_c values. Moreover, the higher the share of lignosulfonamide (e.g., DDA), the more amorphous phase was formed. It is also worth noting that with the appearance of the second melting peak, the nature of the mass loss increased (increased slope of the mass loss curves).

Micro-combustion calorimetry (MCC)

In author previous work [18], it was shown that the obtained lignosulfonamides and calcium lignosulfonate were characterized by two combustion stages: the first in the range of 100–250 s and the second in the range of 250–370 s. Moreover, dibutyl-lignosulfonamides and *N*-butyl-*N*-dodecyl-lignosulfonamides burned the fastest in the range of 300–400°C, while didodecyl-lignosulfonamides burned almost immediately after ignition in the range of 130–280°C. Furthermore, the obtained lignosulfonamides also showed a weak afterburning-char step in the 430–630°C range [18]. It was then found that the obtained biomaterials were characterized by a PHRR coefficient ranging from 13 to 35 W/g, which made them potentially non-flammable. Furthermore, lignosulfonamides con-

T a b l e 2. DSC data of PLA/lignosulfonamide composites

Sample	T_g, °C	ΔCp, J/g·K	T_{cc}, °C	T_{m1}, °C	T_{m2}, °C	ΔH_m, J/g	X_c, %
PLA	64	0.50	122	–	153	23.12	2.80
PLA/CLS3	60	0.96	126	–	153	6.42	1.39
PLA/CLS6	56	0.46	125	–	153	12.76	1.16
PLA/CLS9	57	0.49	126	–	153	10.50	0.97
PLA/DBA3	59	0.60	120	–	150	30.32	1.50
PLA/DBA6	57	0.58	128	148	151	12.77	0.61
PLA/DBA9	55	0.56	127	147	151	10.36	0.72
PLA/NNA3	55	0.60	128	149	152	11.08	0.28
PLA/NNA6	56	0.58	129	149	152	4.81	0.51
PLA/NNA9	56	0.57	128	148	152	4.33	0.39
PLA/DDA3	56	0.62	129	149	152	3.09	0.22
PLA/DDA6	56	0.61	128	148	152	3.81	0.18
PLA/DDA9	55	0.60	127	146	151	4.82	0.05

T_m – melting temperature, ΔH_m – melting enthalpy, ΔC_p - change in the heat capacity, T_{cc} – cold crystallization temperature, T_g – glass transition temperature, X_c – degree of crystallinity, T_c – crystallization temperature.

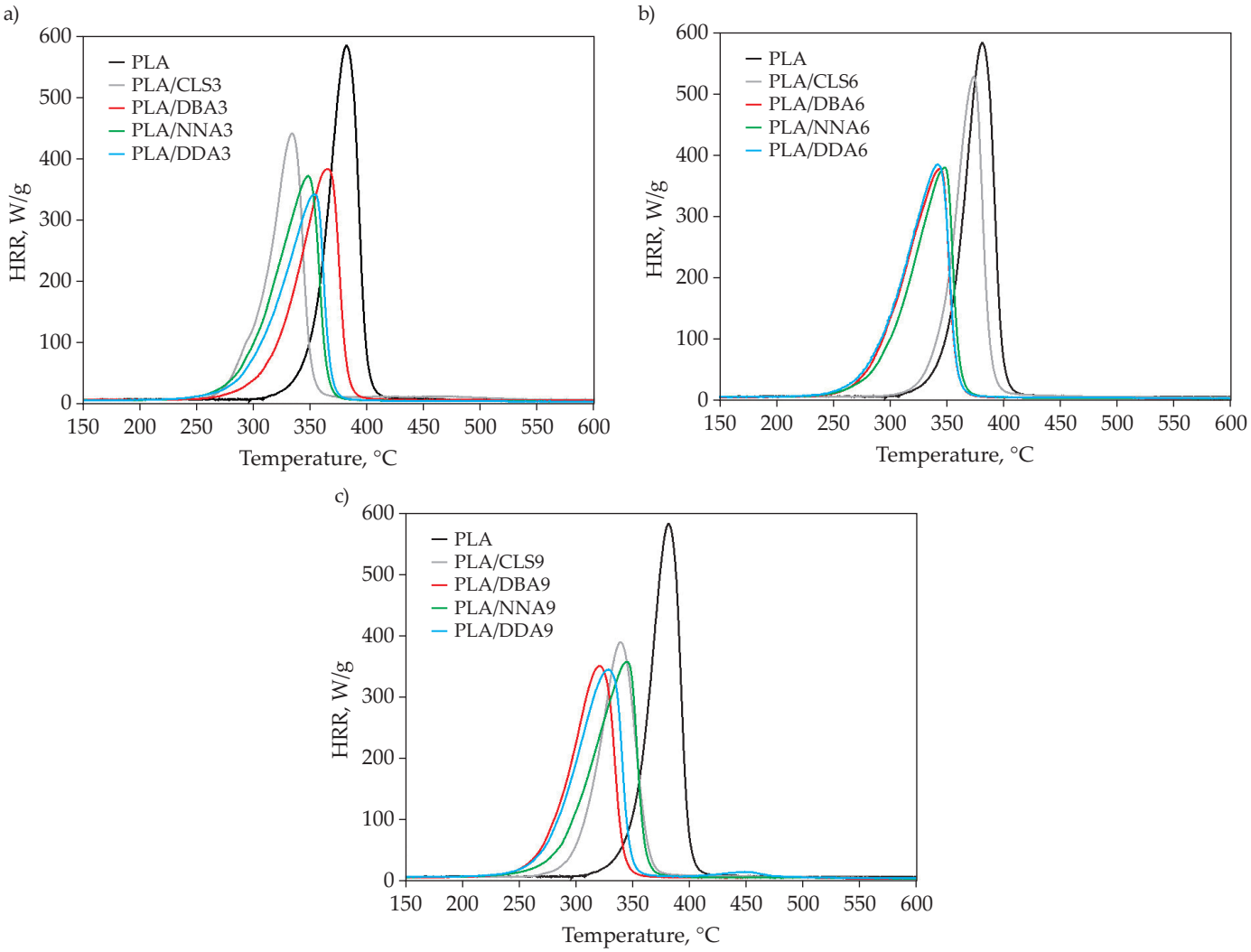

Fig. 4. Heat release rate (HRR) curves for PLA/lignosulfonamide composites with different lignosulfonamide content: a) 3 wt%, b) 6 wt%, c) 9 wt%

T a b l e 3. Flammability indicators for raw materials and hybrid biocomposites

Sample	PHRR W/g	HRR_{AV} W/g	HOC_{AV} kJ/g	THR_{600s} kJ/g	TTI		TOF		Combustion time, s
					s	°C	s	°C	
PLA	584	34	11.64	22.38	268	305	384	423	116
PLA/CLS3	440	31	11.62	20.28	203	253	321	375	118
PLA/CLS6	529	29	10.30	19.45	268	303	368	406	100
PLA/CLS9	390	27	10.55	18.12	216	266	333	386	117
PLA/DBA3	382	30	11.30	20.18	191	243	362	409	171
PLA/DBA6	379	29	11.82	19.99	194	237	333	380	139
PLA/DBA9	352	27	11.12	18.29	158	200	340	384	182
PLA/NNA3	371	29	11.45	19.64	186	228	350	395	164
PLA/NNA6	381	29	11.49	19.46	168	217	332	384	164
PLA/NNA9	358	28	11.25	19.40	177	211	357	393	180
PLA/DDA3	341	27	10.51	18.03	174	222	344	395	170
PLA/DDA6	386	31	12.52	21.06	169	217	333	386	164
PLA/DDA9	345	29	11.97	19.87	172	220	321	371	149

PHRR – peak of heat released rate, HRR_{AV} – average heat released rate, HOC_{AV} – average heat of combustion, THR_{600s} – total heat released after 600 s, TTI – time to ignition, TOF – time out flame.

taining two long aliphatic chains with 12 carbon atoms were found to be more susceptible to decomposition at high temperatures than those containing two butyl chains or one C_4 and one C_{12} chain. It was proved that *N*-butyl-*N*-dodecyl-lignosulfonamides released small amounts of heat, burned slowly, and produced intermediate amounts of solid residues [18].

The promising properties of the obtained lignosulfonamides were assessed for reducing the flammability of PLA. The results of the MCC analysis of the PLA/CLS and PLA/lignosulfonamide composites and the reference sample are presented in Figure 4, and the indicators collected because of this analysis are presented in Table 3.

Pure PLA burned in less than 120 s, emitting an average of 11.64 kJ/g of heat. The maximum heat release rate (PHRR) was recorded at 382°C, equal to 584 W/g [20].

The addition of 9 wt% CLS reduced PHRR more than 30% compared to PLA but maintained a similar combustion time. PLA/CLS composites also ignited faster and extinguished earlier than the reference sample. The high content of CLS increased PLA's susceptibility to ignition at lower temperatures even though a high flame retardant effect of the biomaterial was achieved.

The use of any of the synthesized lignosulfonamides in the amount of 3 wt% allowed for a greater reduction of PHRR than 9 wt% CLS. However, the use of 9 wt% DBA resulted in a PHRR of 352 W/g, which is 40% lower compared to PLA. PLA/DBA composites burned very similarly to PLA/CLS. A similar trend was observed in the changes of the total heat release after 600 s (THR_{600s}) and average heat release rate (HRR_{AV}), decreasing with the increase in the lignosulfonamide content in PLA. Also in both cases, composites containing 6 wt% of HFFR (PLA/CLS6 and PLA/DBA6) burned the fastest. It can be concluded that biocomposites showing the best effect of reducing flammability ignited much earlier than the reference sample, not necessarily burning the longest. In the case of PLA/NNA composites, the difference between the combustion of samples containing 3 and 6 wt% lignosulfonamide was small. Similar values of HRR_{AV}, HOC_{AV}, and THR_{600s} indices were obtained, with about a 35% reduction in flammability and even identical total combustion time. The best results among PLA/NNA composites were obtained by the sample containing 9 wt% of lignosulfonamide (39% reduction in PHRR index compared to PLA). This composite had one of the longest burning times (180 s). The use of 3 wt% DDA resulted in the highest (42%) PHRR reduction in relation to PLA. A similar result was also obtained for the PLA/DDA9 composite, which allowed for the 41% reduction. Thus, PLA/DDA3 and PLA/DDA9 samples were characterized by similar HRR_{AV}, HOC_{AV}, THR_{600s}, or TTI values (Table 3). They differed, among other things, in combustion time, which resulted from the PLA/DDA3 sample extinguishing faster by about 20 s.

The flammability of PLA/lignosulfonamide composites was mostly dependent on the type of lignosulfonamide used in the sample, and only secondary on its mass fraction. The lowest flammability was achieved by composites containing DDA. In turn, PLA/DBA and PLA/NNA composites burned very similarly and the introduction of the lignosulfonamide fraction criterion did not allow for an unequivocal statement as to which additive was better. Considering each type of lignosulfonamide separately, the analyzed composites can be classified in terms of flammability as follows:

T a b l e 4. Flammability factors for PLA biocomposites calculated according to ASTM D7309

Sample	Q_{max}, W/g	$T_{5\%}$		$T_{95\%}$		FGC, J/gK	η_c, J/gK	h_c, kJ/g	$h_{c\,gas}$, kJ/g	Y_P, %
		s	K	s	K					
PLA	584	243	552	495	811	179	650	22.90	22.90	0
PLA/ CLS3	440	211	535	544	876	150	478	20.94	22.94	0
PLA/ CLS6	529	244	552	514	829	151	590	19.99	18.74	6
PLA/ CLS9	390	210	533	458	787	151	428	18.43	16.29	12
PLA/ DBA3	382	221	538	500	823	158	422	20.68	19.44	6
PLA/ DBA6	379	216	533	388	710	201	418	20.25	20.25	0
PLA/ DBA9	352	209	523	426	745	166	390	18.56	18.56	0
PLA/ NNA3	371	218	534	420	741	181	412	19.95	17.87	10
PLA/ NNA6	381	206	528	416	743	178	418	19.74	16.80	15
PLA/ NNA9	358	219	525	452	764	170	402	19.77	19.77	0
PLA/ DDA3	341	206	527	419	744	164	375	18.29	18.29	0
PLA/ DDA6	386	209	531	426	754	188	423	21.38	20.09	6
PLA/ DDA9	345	200	521	447	773	171	381	20.21	19.36	4

FGC – fire growth capacity of sample, h_c – specific heat release in the test, η_c – heat release capacity, $T_{5\%}$ - temperature in the test at which 5 % of h_c has been released measured at a heating rate β = 1 K/s, $T_{95\%}$ - temperature in the test at 95 % of h_c has been released measured at a heating rate β = 1 K/s, $h_{c\,gas}$ – specific heat of gases combustion, Y_P – pyrolysis residue.

a) PLA/CLS9 < PLA/CLS3 <<< PLA/CLS6
b) PLA/DBA9 < PLA/DBA3 = PLA/DBA6
c) PLA/NNA9 < PLA/NNA3 = PLA/NNA6
d) PLA/DDA3 = PLA/DDA9 <<< PLA/DDA6

This means that the synthesized lignosulfonamides were effective mostly at high content (9 wt%), although there were cases where, when using a compound containing long aliphatic chains in the structure, a lower lignosulfonamide content of 3 wt% was sufficient.

MCC vs TGA

To assess in detail the flammability of the obtained PLA/lignosulfonamide composites, additional flammability indices were determined by the ASTM D7309 standard. Table 4 contains a summary of the following indices: heat release capacity (η_c), specific heat release in the test (h_c), fire growth capacity of the sample (FGC), the specific heat of gas combustion ($h_{c\,gas}$), and pyrolysis residue (Y_P). The values of indicators such as: η_c, FGC, Y_P, $h_{c\,gas}$ were calculated according to Equations 2–5:

$$\eta = \frac{Q_{max}}{\beta} \tag{2}$$

$$FGC = \frac{h_v}{T_{5\%} - T_0} + \frac{h_c}{T_{95\%} - T_0} \tag{3}$$

$$Y_P = \frac{m_p}{m_0} \tag{4}$$

$$h_{c\,gas} = \frac{h_c}{1 - Y_P} \tag{5}$$

where: Q_{max} – PHRR (W/g), β – average heating rate over the measurement range (K/s), $T_{5\%}$ – temperature in the test at which 5% of h_c has been released measured at a heating rate 1 K/s, $T_{95\%}$ – temperature in the test at 95% of h_c has been released measured at a heating rate 1 K/s, T_0 – standard room temperature (K), m_p – residual specimen mass after the anaerobic pyrolysis (g), m_0 – initial specimen mass (g).

FGC is a parameter that allows for the assessment of fire development using data obtained at the microscale. High values of FGC, as well as Q_{max}, η_c, and h_c, indicate the high flammability of a given material and the ability of the biomaterial to potentially spread the fire further. As can be seen in Table 4, such materials primarily include the reference sample (PLA). Importantly, the PLA/lignosulfonamide composite samples with the lowest PHRR values were also characterized by the lowest heat

release capacity (η_c), while having a fire spread capacity that was not much lower than PLA (up to 8%). In addition, PLA/DBA6 and PLA/DDA6 composites were more susceptible to flame spread than PLA, although the heat release effect was small. This is partly related to the char formation mechanism, as it was observed that with increasing solid residue the total heat release (THR) value decreased (especially when using lignosulfonamides containing long aliphatic chains).

The effect of synthesized lignosulfonamides and calcium lignosulfonate on the thermal stability and flammability of PLA was also compared, which was achieved by determining the values of the overall thermal stabilization effect (OSE) and the overall fire retardancy effect (OFRE). The OSE and OFRE indices were determined using Equations 6 and 7 [23, 25, 26]:

$$OSE = \sum_{T=150}^{600} [(\text{mass percent of polymer material}_T) + - (\text{mass percent of polylactide}_T)] \quad (6)$$

$$OFRE = \sum_{T=150}^{600} [(\text{HRR percent of polylactide}_T) + - (\text{HRR percent of polymer material}_T)] \quad (7)$$

The OSE and OFRE coefficients are values related to PLA. Their comparison shown in Figure 5 confirms the previous results of the TGA and MCC analyses.

The results show that only PLA/CLS composites had improved thermal stability compared to PLA and simultaneously reduced flammability. Moreover, with the increase of CLS content in PLA, the OSE value decreased in favor of the increase of OFRE. The reason for this is the possibility of CLS to slight coke, especially in the range of 387–507°C, which increases with the increase of the amount of CLS in the sample. Because in this range, the final decomposition of lignin to a solid residue occurs. The general rule is that the more solid residue is formed, the greater the flame retardant effect is achieved.

The effect of synthesized lignosulfonamides on OSE and OFRE of biocomposites was discussed separately

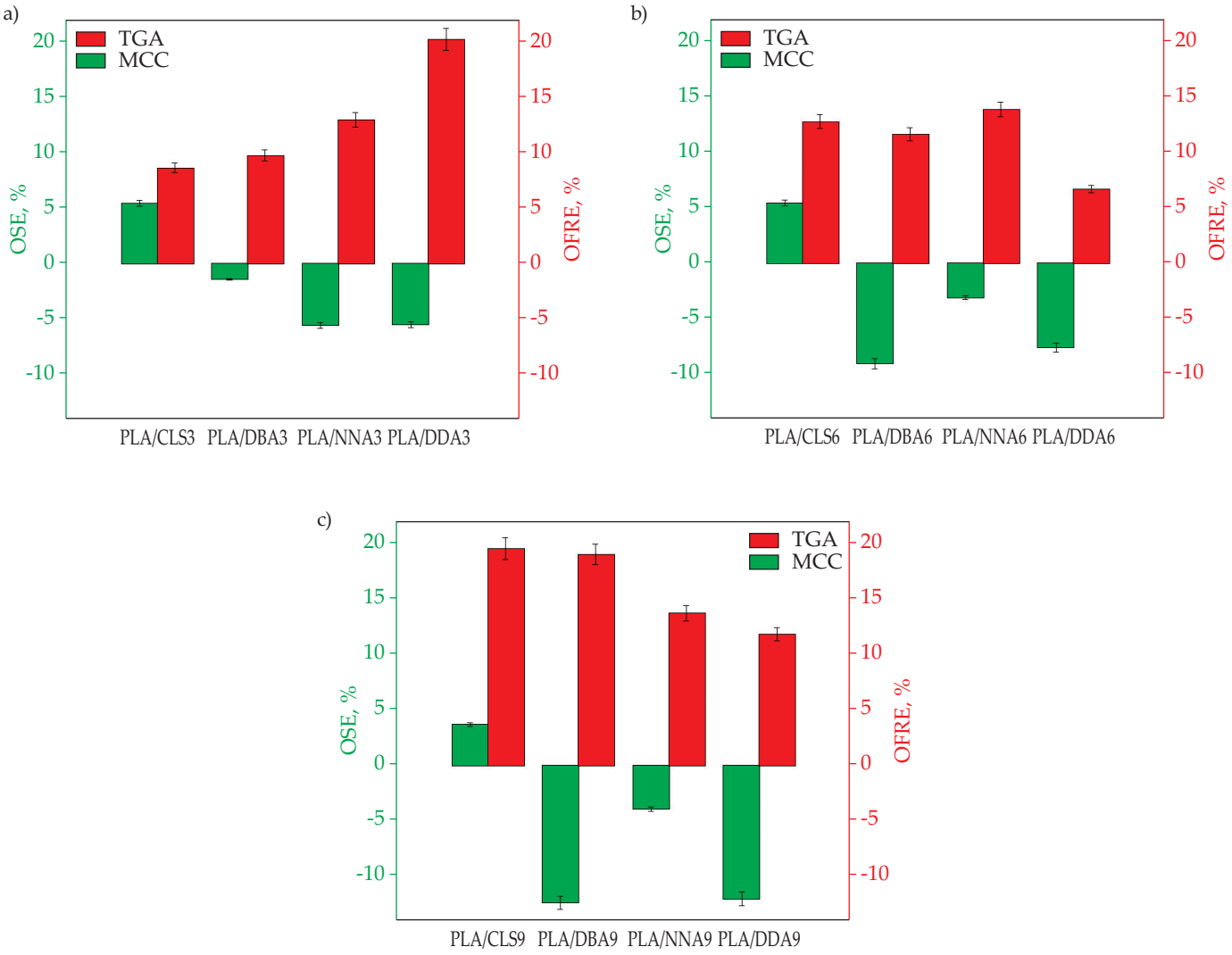

Fig. 5. OSE and OFRE for PLA/lignosulfoamide biocomposites with different lignosulfonamide content: a) 3 wt%, b) 6 wt%, c) 9 wt%

for each HFFR mass fraction. For the PLA/lignosulfonamide biocomposites shown in Figure 5a, an almost perfect example of the relationship between OSE and OFRE was obtained. The thermal stability of the biocomposites decreased with increasing aliphatic chain lengths in the lignosulfonamide structure. This means that the biocomposites containing lignosulfonamide rich in C_{12} chains were more prone to char formation. At the same time, with decreasing thermal stability, OFRE increased. With the increase in lignosulfonamide content, this relationship was completely disrupted (Figure 5b and c). In both cases (6 and 9 wt%), the use of NNA gave a similar trend - a slightly negative OSE and high OFRE. In turn, the use of DBA and DDA (2 short and 2 long aliphatic chains in the structure) gave a different trend from the previous one - a high negative OSE and high OFRE. Unfortunately, also a higher lignosulfonamide content resulted in the PLA/DDA composites having the worst OFRE values in the individual comparison. Thus, the comparison of composites in terms of thermal stability based on the OSE index should be adjusted accordingly: PLA/CLS3 = PLA/CLS6 > PLA/CLS9 > PLA/DBA3 > PLA/NNA6 > PLA/NNA9 > PLA/DDA3 > PLA/NNA3 > PLA/DDA6 > PLA/DBA6 > PLA/DDA9 > PLA/DBA9. The series of samples in bold in the above list coincides with the series presented in previous section. Similar comparison of composites in terms of flammability based on OFRE index was corrected as follows:

PLA/CLS9 <<< PLA/CLS6 < PLA/CLS3
PLA/DBA9 <<< PLA/DBA6 < PLA/DBA3
PLA/NNA9 = PLA/NNA6 < PLA/NNA3
PLA/DDA3 <<< PLA/DDA9 < PLA/DDA6

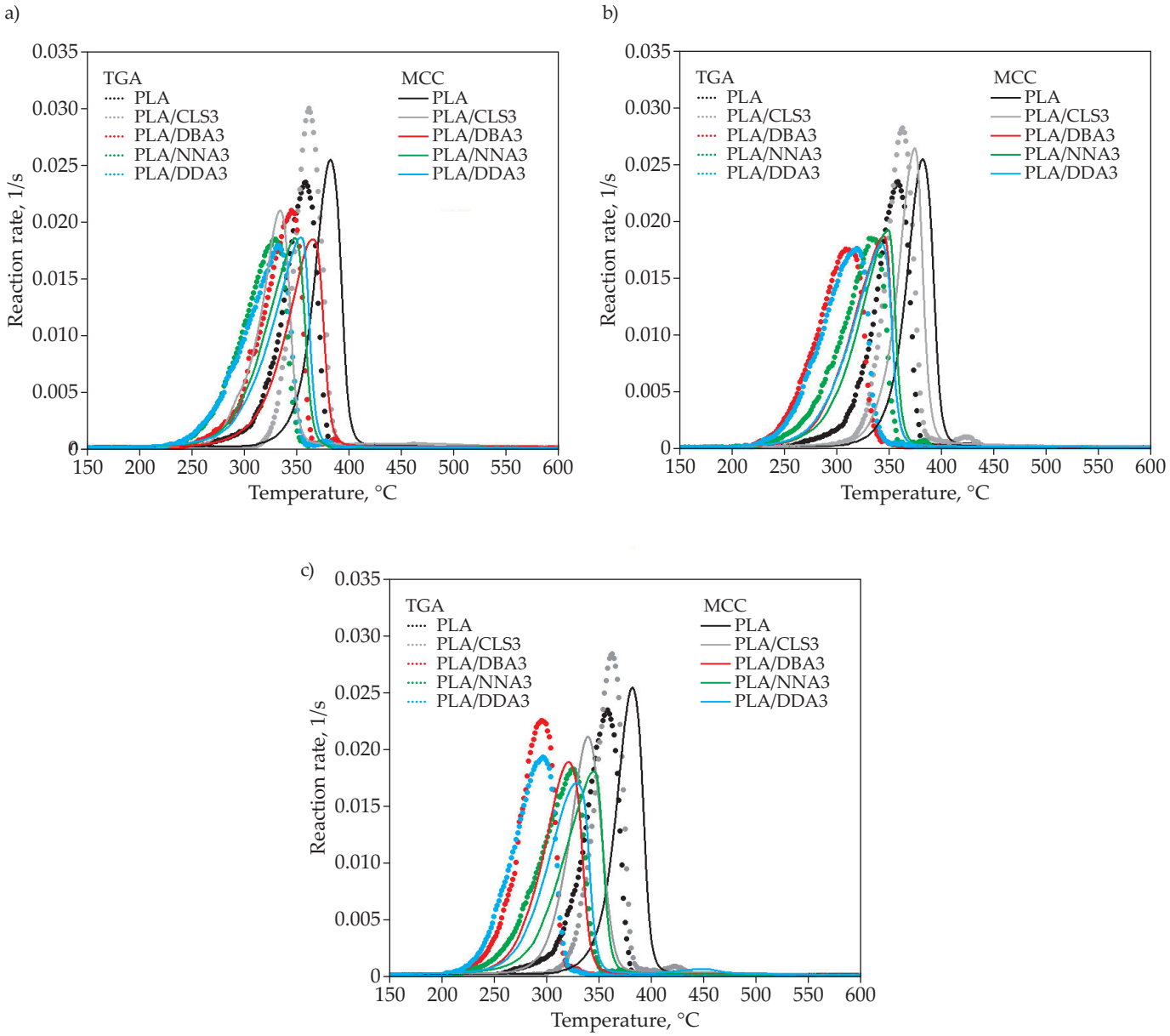

Fig. 6. Reaction rate calculated from TGA and MCC results for PLA/CLS and PLA/lignosulfonamide biocomposites with different lignosulfonamide content: a) 3 wt%, b) 6 wt%, c) 9 wt%

T a b l e 5. List of PLA flammability reducing additives examined by authors

Type of composite	Type of additive	Amount of additive, wt%	Flammability reduction, %	Reference
PLA/DDA	Didodecyl-lignosulfonamide	3	42	This study
PLA/DBA	Dibutyl-lignosulfonamide	9	40	This study
PLA/NNA	*N*-butyl-*N*-dodecyl-lignosulfonamide	9	39	This study
PLA/EC	*Elettaria Cardamomum L.*	10	37	[36]
PLA/CLS	Calcium lignosulfonate	9	33	[20]
PLA/TA	Tannic acid	9	30	[20]
PLA/BMT	Tannic acid adsorbed on calcium lignosulfonate	6	30	[20]
PLA/MF	*Myristica fragrans Houtt.*	7.5	29	[36]
PLA/SF-BMIC	Pyrolyzed montmorillonite purified with 1-butyl-3-methylimidazolium chloride	5	23	[25]
PLA/SF-BMAC	Pyrolyzed montmorillonite purified with methyldodecylbenzyl trimethyl ammonium chloride	5	23	[25]
15BL(PLA/NS)	Composite coated with bilayers consists of chitosan and nanosilica	15 bilayers	22	[24]
PLA/UD	*Urtica dioica* fibers	15	20	[41]
PLA/MUD	*Urtica dioica* fibers treated with a 10% NaOH solution	10	20	[41]
PLA/MVV	*Vitis vinifera* fibers treated with a 10% NaOH solution	5	20	[41]
PLA/VV	*Vitis vinifera* fibers	5	19	[41]
PLA/NS	Nanosilica	5	16	[24]
PLA/MMT	Montmorillonite	5	5	[25]

Based on the procedure proposed in [27], for TGA and MCC data, the reaction rates were calculated from Equations 8 and 9:

$$RR_{TGA} = -\frac{dm/dt}{(m_0 - m_\infty)} \quad (8)$$

$$RR_{MCC} = \frac{\dot{q}}{\dot{\Delta q}} \quad (9)$$

where: RR_{TGA} – the reaction rate of weight loss (s^{-1}), dm/dt – weight derivative over time, m_0 – initial mass of sample (kg), m_∞ – final mass of sample (kg), RR_{MCC} – the reaction rate of heat release (s^{-1}), – specific heat release rate (W/g), – total heat of combustion per unit mass of sample (J/g).

The indicators summarized in Table 5 allows to determine the rate of decomposition reaction (*RR*) (Figure 6) [28–30]. When analyzing the decomposition reaction rate (*RR*) of PLA/lignosulfonamide composites, it should be noted that the amount of the additive did not reflect the peak intensity, but the range of temperatures at which the decomposition process occurred. The difference between the temperature range of the reaction rate (*RR*) curves of PLA decomposition, determined for heating at 10°C/min, and combustion at 1°C/s was only 24°C. This was related to the conditions of the single-stage biopolymer gasification process. Calcium lignosulfonate reversed the trend, i.e., PLA/CLS composites decomposed at higher temperatures during TGA tests than during combustion, maintaining the difference at the level of the RR curves analyzed for PLA. This was the only such case in the considered set, for which the oxidation process of the resulting gaseous compounds was responsible.

With the increase in the share of DBA, the temperature at which the peak of the decomposition reaction rate was read during both TGA and MCC tests shifted towards lower values. Regardless of the amount of NNA used and the heating rate, PLA/NNA composites decomposed in a similar temperature range. This range was always shifted by ~20°C in favor of combustion. The presence of two C12 chains in the DDA structure did not have a significant effect on the decomposition rate of PLA composites. At lower DDA filling, the distances between the temperatures at which the peaks of both RR curves occurred were constant and amounted to 22°C. It should be emphasized that with the increase of the mass fraction of DDA in the composite, the decomposition processes conducted in both the TGA and MCC tests shifted away from the reference sample towards lower temperatures. Only PLA/CLS and PLA/DBA composites had higher reaction rate values during TGA analysis than MCC. The remaining composites decomposed at a similar rate.

The literature states that the nitrogen-sulfur core present in sulfonamides is responsible for reducing the flammability of polymeric materials [31–33]. This is because heating breaks the bond between sulfur and nitrogen. The remaining amide group then decomposes, releasing nitrogen gas. In the process of oxidation of the sulfonate group, an acidic SO_2 compound is released, which promotes the formation of char during the combustion of the PLA matrix [34]. The flame retardancy mechanism is related to the transfer of free radicals on the carbon

planes of the forming amorphous carbon (a-C) [35, 36]. The formed ordered a-C planes, in turn, act synergistically with other compounds present in the system, forming effective flame retardant coatings [37, 38].

Table 5 presents the best results achieved in the author's previous works, where the results of this study were also included in the ranking (bold font). The percentage reduction of the PHRR index of the tested material relative to PLA was assumed as the reduction in flammability. According to the literature [39, 40], the PHRR index can be considered as a comparable level of flammability of a given material relative to the reference sample. It turned out that the use of DBA, NNA, and DDA fillers allowed for obtaining the best results among all the research works indicated in the ranking below.

CONCLUSIONS

This work aimed to check the effectiveness of reducing flammability by synthesized lignosulfonamides. There were indications that the sulfonamide group in the system decomposes with the release of SO_2, which is responsible for char formation. Additionally, the remaining part of lignin played a role in stabilizing the system, especially at higher temperatures. The above expectations were confirmed. TGA analysis showed that the main stage of degradation (up to 400°C) was associated with the oxidation of CO, CO_2, SO_2, and other low-molecular-weight compounds.

On the other hand, the second stage of decomposition was associated with the afterburning of the remaining part of lignin. The best thermal stability was characterized by composites containing pure calcium lignosulfonate (CLS). All PLA/lignosulfonamide composites decomposed earlier than PLA. The type of lignosulfonamide used also influenced the thermo-oxidative decomposition: with the increase in the length of aliphatic chains in the structure, the thermal stability decreased.

Microcalorimetric analysis showed that the compounds of natural origin used allowed to achieve a previously unseen effect of reducing flammability. Composites containing 9 wt% of lignosulfonamide were characterized by about 40% reduction of the PHRR index. However, a six-fold increase in the heating rate caused the samples, instead of forming a stable solid residue, to form coke entrained by escaping gaseous products.

ACKNOWLEDGEMENTS

This research was funded in whole by National Science Centre, Poland, Miniatura 6 Grant No. 2022/06/X/ST5/00004.

Authors contribution

T.M.M. – conceptualization, methodology, validation, formal analysis, data curation, investigation, writing-original draft, writing-review and editing, visualization; Z.Z. – writing-original draft, writing-review and editing; R.P. – writing-original draft, writing-review and editing.

Funding

This research was funded in whole by National Science Centre, Poland, Miniatura 6 Grant No. 2022/06/X/ST5/00004.

Conflict of interest

The authors declare no conflict of interest.

REFERENCES

[1] Shen C., Shao R., Wang W. *et al.*: *European Polymer Journal* **2024**, *220*, 113478. https://doi.org/10.1016/j.eurpolymj.2024.113478

[2] Yin X., Li L., Pang H. *et al.*: *RSC Advances* **2022**, *12*, 14509. https://doi.org/10.1039/D2RA01822E

[3] Lee Y.X., Wang W., Lei Y. *et al.*: *Progress in Organic Coatings* **2025**, *198*, 108903. https://doi.org/10.1016/j.porgcoat.2024.108903

[4] Lu S.Y., Hamerton I.: *Progress in Polymer Science* **2002**, *27*, 1661. https://doi.org/10.1016/S0079-6700(02)00018-7

[5] Sharma V., Agarwal S., Mathur A. *et al.*: *Journal of Industrial and Engineering Chemistry* **2024**, *133*, 38. https://doi.org/10.1016/j.jiec.2023.12.010

[6] Gupta R., Singh M.K., Rangappa S.M. *et al.*: *Heliyon* **2024**, *10(21)*, e39662. https://doi.org/10.1016/j.heliyon.2024.E39662

[7] Rong G., Chen Y., Wang L. *et al.*: *Journal of Applied Polymer Science* **2014**, *131(6)*, 39699. https://doi.org/10.1002/app.39699

[8] Charoeythornkhajhornchai P., Samthong C., Somwangthanaroj A.*: Journal of Applied Polymer Science* **2017**, *134(19)*, 44822. https://doi.org/10.1002/app.44822

[9] Achuenu C., Carret S., Poisson J.F. *et al.*: *European Journal of Organic Chemistry* **2020**, *2020(37)*, 5901. https://doi.org/10.1002/ejoc.202000608

[10] Gigant N., Drège E., Retailleau P. *et al.*: *Chemistry – A European Journal* **2015**, *21(44)*, 15544. https://doi.org/10.1002/chem.201502816

[11] Richards-Taylor C.S., Martínez-Lamenca C., Leenaerts J.E. *et al.*: *Journal of Organic Chemistry* **2017**, *82(18)*, 9898. https://doi.org/10.1021/acs.joc.7b01628

[12] Ma L.J., Li G.X., Huang J. *et al.*: *Tetrahedron Letters* **2018**, *59(48)*, 4255.

https://doi.org/10.1016/j.tetlet.2018.10.038
[13] Rosas-Hernández A., Steinlechner C., Junge H. et al.: "Photo- and Electrochemical Valorization of Carbon Dioxide Using Earth-Abundant Molecular Catalysis" in "Chemical Transforrmation of Carbon Dioxide" (edit. Wu X.F., Beller M.), Springer, Cham 2018. p. 229. https://doi.org/10.1007/978-3-319-77757-3_7
[14] Zhang Y., Liu Y., Ma X. *et al*.: *Dyes and Pigments* **2018**, *158*, 438. https://doi.org/10.1016/j.dyepig.2018.05.073
[15] Sharma D.K., Adams S.T., Liebmann K.L. *et al*.: *Organic Letters* **2019**, *21(6)*, 1641. https://doi.org/10.1021/acs.orglett.9b00173
[16] Parnian R., Soleimani E., Bahrami K.: *Chemistry Select* **2019**, *4(29)*, 8554. https://doi.org/10.1002/slct.201901598
[17] Sohrabnezhad S., Bahrami K., Hakimpoor F.: *Journal of Sulfur Chemistry* **2019**, *40(3)*, 256. https://doi.org/10.1080/17415993.2019.1570196
[18] Majka T.M.: *Polimery* **2023**, *68(10)*, 544. https://doi.org/10.14314/polimery.2023.10.4
[19] Fernández-Pérez M., Flores-Céspedes F., Daza-Fernández I. *et al*.: *Industrial and Engineering Chemistry Research* **2014**, *53(35)*, 13557. https://doi.org/10.1021/ie500186e
[20] Majka T.M., Pimentel A.C., Fernandes S. *et al*.: *Thermochimica Acta* **2024**, *737*, 179769. https://doi.org/10.1016/j.tca.2024.179769
[21] Han H., Li J., Wang H. *et al*.: *Energy and Fuels* **2019**, *33(5)*, 4302. https://doi.org/10.1021/acs.energyfuels.9b00332
[22] Lewis Richard J.: "Sax's Dangerous Properties of Industrial Materials" 12th Edition, John Wiley and Sons, Hoboken 2012.
[23] Majka T.M.: *Journal of Polymer Research* **2023**, *30*, 357. https://doi.org/10.1007/s10965-023-03737-z
[24] Majka T.M.: *International Journal of Heat and Technology* **2024**, *42(4)*, 1257. https://doi.org/10.18280/IJHT.420416
[25] Majka T.M.: *Iranian Polymer Journal* **2024**. https://doi.org/10.1007/s13726-024-01396-5
[26] Majka T.M., Bukowczan A., Pielichowski K.: Journal of Materials Engineering and Performance **2024**, *33*, 13637. https://doi.org/10.1007/s11665-024-10344-6
[27] Snegirev A.Y.: *Thermochimica Acta* **2014**, *590*, 242. https://doi.org/10.1016/j.tca.2014.07.009
[28] Berkowicz G., Majka T.M., Żukowski W.: Energy Conversion and Management **2020**, *214*, 112888. https://doi.org/10.1016/j.enconman.2020.112888
[29] Żukowski W., Berkowicz G., Majka T.M.: *Data in Brief* **2020**, *31*, 105703. https://doi.org/10.1016/j.dib.2020.105703
[30] Majka T.M., Berkowicz-Płatek G., Żukowski W.: *Materials* **2021**, *14(9)*, 2281. https://doi.org/10.3390/ma14092281
[31] Tirri T., Aubert M., Aziz H. *et al*.: *Polymer Degradation and Stability* **2019**, *164*, 75. https://doi.org/10.1016/j.polymdegradstab.2019.03.021
[32] Mountassir A., Tirri T., Sund P. *et al*.: *Polymer degradation and Stability* **2021**, *188*, 109588. https://doi.org/10.1016/j.polymdegradstab.2021.109588
[33] Sai T., Ran S., Guo Z. *et al*.: *SusMat* **2022**, *2(4)*, 411. https://doi.org/10.1002/sus2.73
[34] Yang H., Yue H., Zhao X. *et al*.: *Materials* **2020**, *13(17)*, 3656. https://doi.org/10.3390/ma13173656
[35] Hou B., Shan X., Yin H. *et al*.: *Chemical Engineering Journal* **2024**, *491*, 152186, doi: 10.1016/J.CEJ.2024.152186
[36] Majka T.M: *BioResources* **2024**, *20(1)*, 1655.
[37] Ma H., Fang Z.: *Thermochimica Acta* **2012**, *543*, 130. https://doi.org/10.1016/j.tca.2012.05.021
[38] Ren S., Xu X., Zhu Z.S. *et al*.: *Applied Catalysis B: Environmental* **2024**, *342*, 123410. https://doi.org/10.1016/j.apcatb.2023.123410
[39] Schartel B., Wilkie C.A., Camino G.: *Journal of Fire Sciences* **2016**, *34(6)*, 447. https://doi.org/10.1177/0734904116675881
[40] Schartel B., Wilkie C.A., Camino G: *Journal of Fire Sciences* **2017**, *35(1)*, 3. https://doi.org/10.1177/0734904116675370
[41] Majka T.M., Piech R., Piechaczek M. *et al*.: *Materials* **2024**, *17(6)*, 1256. https://doi.org/10.3390/ma17061256

Received 15 X 2024.
Accepted 5 XI 2024.